J|A|C|S
ARTICLES
Published on Web 03/12/2003

Model Studies of DNA C5′ Radicals. Selective Generation and Reactivity of 2′-Deoxyadenosin-5′-yl Radical

Chryssostomos Chatgilialoglu,* Maurizio Guerra, and Quinto G. Mulazzani

Contribution from the ISOF, Consiglio Nazionale delle Ricerche, Via P. Gobetti 101, 40129 Bologna, Italy

Received November 17, 2002; E-mail: chrys@isof.cnr.it

Abstract: The reaction of hydrated electrons (e_{aq}^-) with 8-bromo-2′-deoxyadenosine has been investigated by radiolytic methods coupled with product studies and addressed computationally by means of DFT-B3LYP calculations. Pulse radiolysis revealed that this reaction was complete in ~0.3 μs, and, at this time, no significant absorption was detected. The spectrum of a transient developed in 20 μs has an absorbance in the range 300−500 nm ($\epsilon_{max} \cong 9600$ M^{-1} cm^{-1} at 360 nm), and it was assigned to aromatic aminyl radical **3**. Computed vertical transitions (TD-UB3LYP/6-311+G*) are in good agreement with the experimental observations. Radical **3** is obtained by the following reaction sequence: one-electron reductive cleavage of the C−Br bond that gives the C8 radical, a fast radical translocation from the C8 to C5′ position, and an intramolecular attack of the C5′ radical at the C8,N7 double bond of the adenine moiety. The rate constant for the cyclization is 1.6×10^5 s^{-1}. On the basis of the theoretical findings, the cyclization step is highly stereospecific. The rate constants for the reactions of C5′ and aminyl **3** radicals with different oxidants were determined by pulse radiolysis methods. The respective rate constants for the reaction of 2′-deoxyadenosin-5′-yl radical with dioxygen, $Fe(CN)_6^{3-}$, and MV^{2+} in water at ambient temperature are 1.9×10^9, 4.2×10^9, and 2.2×10^8 M^{-1} s^{-1}. The value for the reaction of aminyl radical **3** with $Fe(CN)_6^{3-}$ is 8.3×10^8 M^{-1} s^{-1}, whereas the reaction with dioxygen is reversible. Tailored experiments allowed the reaction mechanism to be defined in some detail. A synthetically useful radical cascade process has also been developed that allows in a one-pot procedure the conversion of 8-bromo-2′-deoxyadenosine to 5′,8-cyclo-2′-deoxyadenosine in a diastereoisomeric ratio (5′*R*):(5′*S*) = 6:1 and in high yield, by reaction with hydrated electrons in the presence of $K_4Fe(CN)_6$.

Introduction

Apart from the usual glycosidic bond in 5′,8-cyclopurine-2′-deoxynucleosides, there is an additional base-sugar linkage between the C8 position of purine and the C5′ position of the 2-deoxyribose (cf. Scheme 1). The cyclopurine lesions are observed among the decomposition products of DNA, when exposed even to moderate doses of ionizing radiations, and their percentage levels are comparable to the two major lesions, that is, 8-oxo-7,8-dihydroguanine and thymine glycol.[1−6] These lesions, when formed in DNA, could have a significant biological impact on the conformation and function of the double helix.[7−10] When DNA, oligonucleotides, or nucleosides are exposed to hydroxyl radicals, abstraction of the hydrogen occurs

Scheme 1

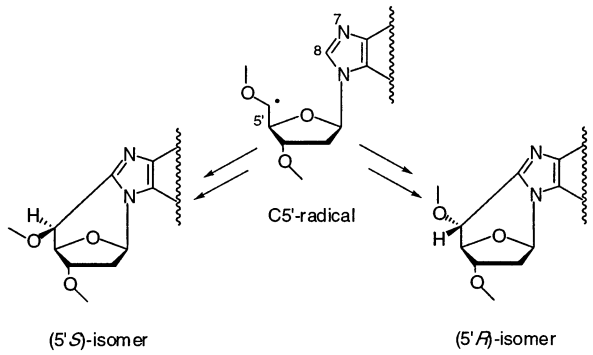

(1) Dirksen, M.-L.; Brakely, W. F.; Holwitt, E.; Dizdaroglu, M. *Int. J. Radiat. Biol.* **1988**, *54*, 195−204. Dizdaroglu, M.; Dirksen, M.-L.; Jiang, H.; Robbins, J. H. *Biochem. J.* **1987**, *241*, 929−932.
(2) Dizdaroglu, M.; Jaruga, P.; Rodriguez, H. *Free Radical Biol. Med.* **2001**, *30*, 774−784.
(3) Jaruga, P.; Birincioglu, M.; Rodriguez, H.; Dizdaroglu, M. *Biochemistry* **2002**, *41*, 3703−3711.
(4) In polyadenylic acid, see: Fuciarelli, A. F.; Miller, G. G.; Raleigh, J. A. *Radiat. Res.* **1985**, *104*, 3272−283. Fuciarelli, A. F.; Shum, F. Y.; Raleigh, J. A. *Biochem. Biophys. Res. Commun.* **1986**, *134*, 883−887. Fuciarelli, A. F.; Shum, F. Y.; Raleigh, J. A. *Radiat. Res.* **1987**, *110*, 35−44.
(5) It is worth mentioning that the formation of 5′,8-cyclopurine nucleosides was first discovered to take place in 5′-AMP upon hydroxyl radical attack. See: Keck, K. *Z. Naturforsch.* **1968**, *23B*, 1034−1043. Raleigh, J. A.; Kremers, W.; Whitehouse, R. *Radiat. Res.* **1976**, *65*, 414−422. Raleigh, J. A.; Fuciarelli, A. F. *Radiat. Res.* **1985**, *102*, 165−176. Haromy, T. P.; Raleigh, J.; Sundaralingam, M. *Biochemistry* **1980**, *19*, 1718−1722.
(6) For some reviews, see: Dizdaroglu, M. *Free Radical Biol. Med.* **1991**, *10*, 225−242. Breen, A. P.; Murphy, J. A. *Free Radical Biol. Med.* **1995**, *18*, 1033−1077. Burrows, C. J.; Muller, J. G. *Chem. Rev.* **1998**, *98*, 1109−1151. Chatgilialoglu, C.; O'Neill. P. *Exp. Gerontol.* **2001**, *36*, 1459−1471.
(7) Kuraoka, I.; Bender, C.; Romieu, A.; Cadet, J.; Wood, R. D.; Lindahl, T. *Proc. Natl. Acad. Sci. U.S.A.* **2000**, *97*, 3832−3837.
(8) Brooks, P. J.; Wise, D. S.; Berry, D. A.; Kosmoski, J. V.; Smerdon, M. J.; Somers, R. L.; Mackie, H.; Spoonde, A. Y.; Ackerman, E. J.; Coleman, K.; Tarone, R. E.; Robbins, J. H. *J. Biol. Chem.* **2000**, *275*, 22355−22362.
(9) Randerath, K.; Zhou, G. D.; Somers, R. L.; Robbins, J. H.; Brooks, P. J. *J. Biol. Chem.* **2001**, *276*, 36051−36057.
(10) Kuraoka, I.; Robins, P.; Masutani, C.; Hanaoka, F.; Gasparutto, D.; Cadet, J.; Wood, R. D.; Lindahl, T. *J. Biol. Chem.* **2001**, *276*, 49283−49288.

mainly at the C4′ and C5′ positions of the sugar moieties.[11] It has been proposed that the C5′ radical might intramolecularly attack the C8,N7 double bond of the adenine or guanine moieties to form 5′,8-cyclopurine nucleotides as the final products (Scheme 1).[1−6,12,13] Cyclopurine deoxynucleosides are formed in two diastereoisomeric forms depending on the configuration at the C5′ position, that is, (5′*S*)- and (5′*R*)-isomers in Scheme 1. Depending on the substrate and the experimental conditions, the ratio of the (5′*S*)- and (5′*R*)-isomers changes substantially. γ-Irradiation of an aqueous solution of 2′-deoxyadenosine[2] or 2′-deoxyguanosine[3] afforded mainly the (5′*R*)-isomers, suggesting a highly stereoselective radical process. The (5′*R*)-isomer was also detected under similar conditions upon irradiation of tetranucleotide d(ApCpGpT).[14] Regarding the effect of DNA conformation, (5′*R*):(5′*S*) ratios of approximately 2 and 0.3 were recently reported by Dizdaroglu and co-workers for cyclodeoxyadenosine and cyclodeoxyguanosine, respectively, in double-stranded DNA,[2,3] whereas the (5′*R*)-isomer of both compounds was found to predominate in single-stranded DNA.[1] It is worth also mentioning that the yields of cyclopurine nucleosides in single-stranded DNA were higher than those in double-stranded DNA and that the cyclodeoxyadenosines are more abundant than cyclodeoxyguanosines.[1]

Cadet and co-workers recently prepared (5′*S*)-5′,8-cyclo-dAdo in seven steps starting from N^6-benzoyl-dAdo in an overall yield <10%,[15,16] following the strategy developed by Matsuda et al. for the synthesis of the ribo analogue.[17] The preparation of (5′*R*)-5′,8-cyclo-dAdo was achieved by two further steps, involving inversion of configuration at the C5′ position.[18] Synthetic oligonucleotides that contain these modified derivatives at selected sites were also prepared to investigate the biochemical and biophysical features of such lesions.[8,15,18] Indeed, recent experiments indicated that neither the (5′*S*)- nor the (5′*R*)-isomer is recognized by human DNA glycosylases active in the base excision repair pathway.[7,8] The role of nucleotide excision repair was also studied, and both isomers were found to be relatively poor substrates, the (5′*S*)-isomer being repaired more efficiently than the (5′*R*)-isomer.[7,8] The (5′*S*)-isomer was found to be a strong block to gene expression in Chinese hamster ovary and human cells.[8] It was also reported that stereospecific differences between the (5′*S*)- and (5′*R*)-isomer residues affect the relative resistance to exonucleolytic activity and give rise to different efficiencies of translesion synthesis by human polymerase η.[10] Several dinucleotides containing the 5′,8-cyclo-dAdo moiety have also been identified in mammalian cellular DNA in vivo, where its level is enhanced by conditions of oxidative stress.[9] It was suggested that in contrast to several other types of oxidative DNA damage, cyclopurine nucleotides are chemically stable and would be expected to accumulate at a slow rate over years in the DNA, in particular for patients affected by the genetic disease xeroderma pigmentosum, who are unable to carry out nucleotide excision repair.[9,10]

Scheme 2

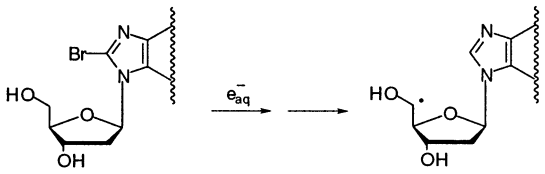

In our laboratory, we envisaged that 8-bromopurine nucleosides were prompt to capture electrons and perhaps rapidly lose the bromine ion to give the corresponding radical in the C8 position,[19,20] which in turn could abstract intramolecularly a hydrogen from the C5′ position to selectively afford the desired C5′ radical (Scheme 2).[21] If our strategy succeeds, we would have an efficient entry to C5′ radical chemistry, starting from 8-bromopurine nucleosides which are also commercially available. Our initial attempt using the 8-bromoguanosine showed that it behaves in a completely different manner.[22] 8-Bromo-dAdo then turned out to be successful, and, in a preliminary communication,[23] we reported the UV−visible spectra of the cyclized aminyl radical and the rate constant for its formation, together with an extraordinary radical cascade reaction that afforded the (5′*R*)-isomer in a one-pot reaction and in excellent yield.[24] We report herein a detailed study which addresses the chemical reactivities of the 2′-deoxyadenosin-5′-yl radical.

Results and Discussion

Reaction of Hydrated Electrons (e_{aq}^-) with 8-Br-dAdo.[16] Radiolysis of neutral water leads to the species e_{aq}^-, HO•, and H• as shown in eq 1 where the values in parentheses represent the radiation chemical yields (*G*-values) in units of μmol/J.[25] The reactions of e_{aq}^- with the substrates were studied by irradiating deareated solutions containing 0.25 M *t*-BuOH. With this amount of *t*-BuOH, HO• is scavenged efficiently (eq 2, $k_2 = 6.0 \times 10^8$ M^{-1} s^{-1}), whereas the H• reacts only slowly.[26] Therefore, the reactions of H• may be relevant because they can account for as much as ∼20% of the products.

$$H_2O \rightsquigarrow e_{aq}^- (0.27), \bullet OH (0.28), \bullet H (0.062) \quad (1)$$

$$HO\bullet + Me_3COH \longrightarrow Me_2C(OH)CH_2\bullet + H_2O \quad (2)$$

The rate constant for the reaction of e_{aq}^- with 8-Br-dAdo was determined by measuring the rate of the optical density

(11) (a) In DNA, abstraction preference for individual hydrogens of the sugar moieties was found in the order H5′ ≈ H4′ > H2′ ≈ H3′ > H1′, see: Pogozelski, W. K.; Tullius, T. D. *Chem. Rev.* **1998**, *98*, 1089−1108. Sy, D.; Savoye, C.; Begusova, M.; Michalik, V.; Charlier, M.; Spotheim-Maurizot, M. *Int. J. Radiat. Biol.* **1997**, *72*, 147−155. (b) Computational data in a simple nucleotide indicate that the most probable sites of H-atom abstraction by radical species are H5′ and H4′ positions, see: Toure, P.; Villena, F.; Melikyan, G. G. *Org. Lett.* **2002**, *4*, 3989−3992.
(12) Marriagi, N.; Cadet, J.; Teoule, R. *Tetrahedron* **1976**, *32*, 2385−2387.
(13) Dizdaroglu, M. *Biochem. J.* **1986**, *238*, 247−254.
(14) Schroder, E. E.; Budzinski, J. C.; Wallace, J. D.; Zimbrick, J. D.; Box, H. C. *Int. J. Radiat. Biol.* **1995**, *68*, 509−523.
(15) Romieu, A.; Gasparutto, D.; Molko, D.; Cadet, J. *J. Org. Chem.* **1998**, *63*, 5245−5249.
(16) dAdo is an abbreviation of 2′-deoxyadenosine, and it will be used throughout the article.
(17) Matsuda, A.; Tezuka, M.; Niizuma, K.; Sugiyama, E.; Ueda, T. *Tetrahedron* **1978**, *34*, 2633−2637.
(18) Romieu, A.; Gasparutto, D.; Cadet, J. *Chem. Res. Toxicol.* **1999**, *12*, 412−421.
(19) For a recent review, see: Savéant, J.-M. In *Advances in Physical Organic Chemistry*; Tidwell, T. T., Ed.; Academic Press: New York, 2000; Vol. 35, pp 117−192.
(20) Such a reaction is well established for bromo derivatives including 5-bromouracil. For example, see: Nese, C.; Yuan, Z.; Schuchmann, M. N.; von Sonntag, C. *Int. J. Radiat. Biol.* **1992**, *62*, 527−541. Sugiyama, H.; Fujimoto, K.; Saito, I. *J. Am. Chem. Soc.* **1995**, *117*, 2945−2946. Cook, G. P.; Greenberg, M. M. *J. Am. Chem. Soc.* **1996**, *118*, 10025−10030. Fujimoto, K.; Sugiyama, H.; Saito, I. *Tetrahedron Lett.* **1998**, *39*, 2137−2140.
(21) This reaction is expected to be ca. 20 kcal/mol exothermic, see: Berkowitz, J.; Ellison, G. B.; Gutman, D. *J. Phys. Chem.* **1994**, *98*, 2744−2765.
(22) Ioele, M.; Bazzanini, R.; Chatgilialoglu, C.; Mulazzani, Q. G. *J. Am. Chem. Soc.* **2000**, *122*, 1900−1908.
(23) Flyunt, R.; Bazzanini, R.; Chatgilialoglu, C.; Mulazzani, Q. G. *J. Am. Chem. Soc.* **2000**, *122*, 4225−4226.
(24) It was reported in a note as unpublished results that photolysis at 254 nm of a deaerated aqueous solution of 8-Br-dAdo afforded (5′*S*)- and (5′*R*)-isomers in 2 and 12% yields, respectively.[15]

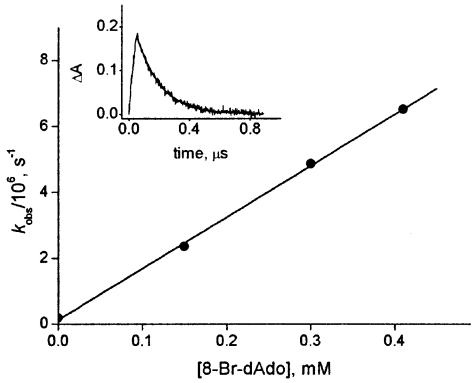

Figure 1. Plot of k_{obs} for the decay of e_{aq}^- at 720 nm as a function of [8-Br-dAdo] in Ar-purged solutions containing 0.25 M *t*-BuOH at pH ≈ 7. Inset: Time dependence of absorption at 720 nm in the presence of 0.41 mM 8-Br-dAdo; optical path = 2.0 cm, dose = 19.3 Gy. The solid line represents the first-order kinetic fit to the data.

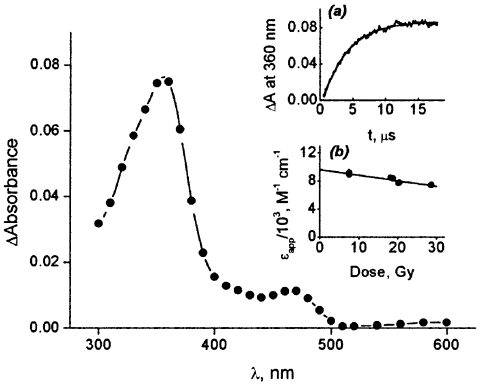

Figure 2. Absorption spectrum obtained from the pulse radiolysis of an Ar-purged solution containing 1 mM 8-Br-dAdo and 0.25 M *t*-BuOH at pH ≈ 7, taken 17 μs after the pulse; dose = 18 Gy, optical path = 2.0 cm. Insets: (a) Time dependence of absorption at 360 nm; the solid line represents the first-order kinetic fit to the data. (b) Dependence of ϵ_{app} (see text) at 360 nm from the radiation dose.

decrease of e_{aq}^- at 720 nm ($\epsilon = 1.9 \times 10^4$ M^{-1} cm^{-1})[27] as a function of nucleoside concentration. Figure 1 (inset) shows the disappearance of e_{aq}^- in the presence of 0.41 mM of 8-Br-dAdo, which leads to a pseudo-first-order rate constant, k_{obs}. From the slope of k_{obs} versus [8-Br-dAdo], the bimolecular rate constant was found to be $(1.6 \pm 0.1) \times 10^{10}$ M^{-1} s^{-1} (Figure 1). As compared with the analogous reaction with dAdo ($k = 8.2 \times 10^9$ M^{-1} s^{-1}),[28] the presence of bromine increased the rate constant of the reduction by a factor of 2.

An aqueous solution of 8-Br-dAdo (1 mM) and *t*-BuOH (0.25 M) at pH ≈ 7 was prepared. Under Ar-purged conditions, the reaction of 8-Br-dAdo with e_{aq}^- was complete in ca. 300 ns. At this time, no significant absorption was detected in the 300−750 nm region. However, a spectrum containing two bands centered at 360 and 470 nm, respectively, developed in ∼20 μs (Figure 2). The time profile for the formation of the transient with $\lambda_{max} = 360$ nm (inset a) followed first-order kinetics with a rate constant (k_{expt}) that was independent of 8-Br-dAdo

Scheme 3

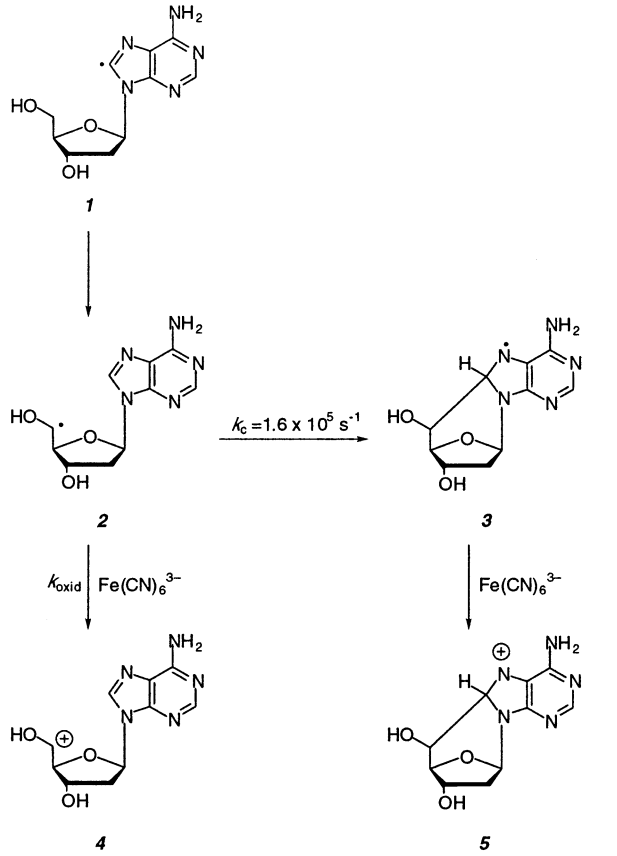

concentration (0.2−1 mM) and slightly increased with dose/pulse. This dose dependence was due to the mixing of first-order growth and second-order decay of the species. By extrapolation to zero dose, a rate constant $k = (1.6 \pm 0.2) \times 10^5$ s^{-1} was obtained. Inset b shows the effect of the dose on the apparent molar extinction coefficient at 360 nm (ϵ_{app}) calculated by assuming a radiation chemical yield $G = 0.27$ μmol/J, which is the G of hydrated electrons.[25] An extinction coefficient of 9600 ± 200 M^{-1} cm^{-1} at 360 nm was calculated by extrapolating to zero dose. For the second peak, an $\epsilon_{470\ nm}$ of ca. 1500 M^{-1} cm^{-1} was calculated. The transient decayed by second-order kinetics with $k/\epsilon_{360\ nm} = 8.8 \times 10^4$ cm s^{-1}.[29]

We assigned the transient shown in Figure 2 to the conjugated aminyl radical **3** and the observed first-order growth to the cyclization of radical **2** (Scheme 3), for the following reasons: (i) The fast reaction of e_{aq}^- with 8-Br-dAdo should afford the aryl radical **1** that has the right geometrical arrangement for a fast exothermic radical translocation to give the C5′ radical **2** (vide infra). (ii) It is well known that neither aryl radical **1** nor α-hydroxylalkyl radical **2** possesses any significant absorbance in the region 300−500 nm;[31] this was also confirmed by the reaction of e_{aq}^- with 8-bromoadenine (without the sugar moiety). (iii) The absorption spectrum in Figure 2 strongly resembles in

(25) Buxton, G. V.; Greenstock, C. L.; Helman, W. P.; Ross, A. B. *J. Phys. Chem. Ref. Data* **1988**, *17*, 513−886 and references therein.
(26) The rate constant of the HO• radical with 8-Br-dAdo was found to be 5.6×10^9 M^{-1} s^{-1} (unpublished work). Therefore, more than 96% of HO• radicals are scavenged by *t*-BuOH when [8-Br-dAdo] ≤ 1×10^{-3} M.
(27) Hug, G. L. *Natl. Stand. Ref. Data Ser., Natl. Bur. Stand.* **1981**, *69*, 6.
(28) Hissung, A.; von Sonntag, C.; Veltwisch, D.; Asmus, K.-D. *Int. J. Radiat. Biol.* **1981**, *39*, 63−71.
(29) The observed second-order kinetics can be assigned to self-termination of aminyl radicals **3** and/or its cross-termination with the $HOC(CH_3)_2CH_2$• radical. Taking into consideration the extinction coefficient, we calculated $k = 8.4 \times 10^8$ M^{-1} s^{-1}, which is similar to the reported self-termination rate constant of $Me_2C(OH)CH_2$• radicals ($k = 6.5 \times 10^8$ M^{-1} s^{-1}).[30]
(30) Ross, A. B.; Mallard, W. G.; Helman, W. P.; Buxton, G. V.; Huie, R. E.; Neta, P. *NDRL-NIST Solution Kinetic Database − Ver. 3*; Notre Dame Radiation Laboratory, Notre Dame, IN and NIST Standard Reference Data, Gaithersburg, MD, 1998 and references therein.
(31) Chatgilialoglu, C. In *Handbook of Organic Photochemistry*; Scaiano, J. C., Ed.; CRC Press: Boca Raton, FL, 1989; Vol. 2, pp 3−11.

shape and ϵ-values that assigned to the isostructural radical **6**, obtained by the reaction of adenine derivatives either with H• or with e_{aq}^- followed by protonation at C8; in the case of adenosine, λ_{max}'s at 355 and 440 nm were observed with extinction coefficients of 10 500 and 1100 M^{-1} cm^{-1}, respectively.[32] The above rationalization was further supported by three experiments: (i) no kinetic isotopic effect was found for the formation of transient by replacing H_2O with D_2O as the reaction medium, (ii) the same spectrum and the same kinetics were obtained by replacing 0.25 M *t*-BuOH with 0.13 M *i*-PrOH, which efficiently trap both H• and HO• species;[33] therefore, H• atoms apparently do not react with 8-Br-dAdo, and (iii) no reaction was observed for H• with 8-Br-dAdo, when the solution was saturated with N_2O to eliminate hydrated electrons. Because H• reacts with adenosine with a rate constant of 2.6×10^8 M^{-1} s^{-1} by adding at the C8 position to give the adduct **6**,[32] probably the presence of bromine substituent at this position either decreases the rate constant substantially or allows the adduct to release Br• rapidly (vide infra).

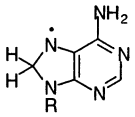

6

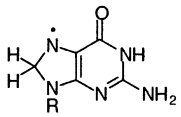

7

Redox Properties of the Transient Species. Useful information on radicals, including the differentiation between isomeric forms, can often be obtained by investigating their reactivity toward so-called redox indicators.[34] The reactivity of the $Fe(CN)_6^{3-}$, $E°[Fe(CN)_6^{3-}/Fe(CN)_6^{4-}] = 0.36$ V,[35] was tested by pulsing deaerated solutions of 1 mM 8-Br-dAdo containing 0.25 M *t*-BuOH and different concentrations of $K_3Fe(CN)_6$ (25−100 μM) at pH 7. Under these conditions, the e_{aq}^- reacted exclusively with 8-Br-dAdo, because $k[e_{aq}^- + Fe(CN)_6^{3-}] = 3.1 \times 10^9$ M^{-1} s^{-1}.[25,30] The absorption at 360 nm was found to decrease by increasing the concentration of $Fe(CN)_6^{3-}$ (see inset of Figure 3). Using a Stern−Volmer type of approach, we obtained $k_{oxid}/k_c = 2.6 \times 10^4$ M^{-1} (Figure 3). The combination of these data with the k_c value yielded $k_{oxid} = 4.2 \times 10^9$ M^{-1} s^{-1}. Because the reaction between the $Me_2C(OH)CH_2$• radical (eq 2) with $Fe(CN)_6^{3-}$ is slow ($k = 3 \times 10^6$ M^{-1} s^{-1}),[36] the decrease of absorption at 360 nm was attributed to a reaction of the C5′ radical **2** with $Fe(CN)_6^{3-}$ (Scheme 3). On the other hand, the disappearance of the transient at 360 nm followed first-order kinetics in the presence of $Fe(CN)_6^{3-}$ (see inset of Figure 4). From the slope of k_{obs} versus $[Fe(CN)_6^{3-}]$, the bimolecular rate constant was found to be $(8.3 \pm 0.3) \times 10^8$ M^{-1} s^{-1} (Figure 4). Scheme 3 summarizes our finding; that is, $Fe(CN)_6^{3-}$ was able to oxidize both the C5′ radical **2** and the aromatic aminyl radical **3**. The resulting cations **4** and **5** could be expected to deprotonate rapidly, affording the corresponding aldehyde and 5′,8-cyclo-dAdo.

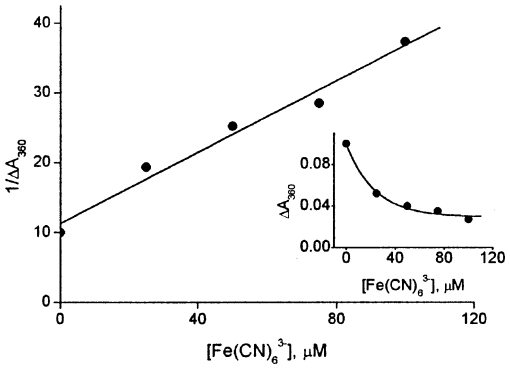

Figure 3. Dependence of 1/ΔAbsorbance at 360 nm on $[Fe(CN)_6^{3-}]$ obtained from the pulse radiolysis of Ar-purged solutions containing 1 mM 8-Br-dAdo and 0.25 M *t*-BuOH at pH ≈ 7; optical path = 2.0 cm, dose = 23.2 Gy. Inset: Dependence of ΔAbsorbance at 360 nm on $[Fe(CN)_6^{3-}]$. The solid line represents an exponential fit to the data.

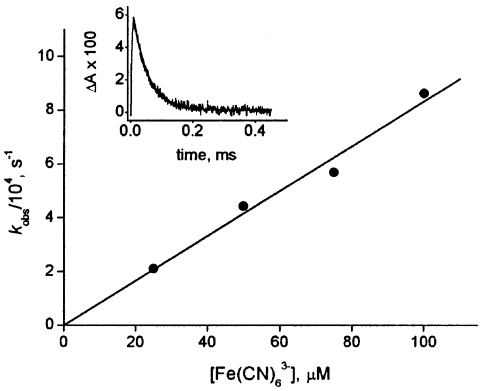

Figure 4. Dependence of k_{obs} for decay at 360 nm on $[Fe(CN)_6^{3-}]$ obtained from the pulse radiolysis of Ar-purged solutions containing 1 mM 8-Br-dAdo and 0.25 M *t*-BuOH at pH ≈ 7. Inset: Time dependence at 360 nm in the presence of 25 mM $[Fe(CN)_6^{3-}]$; optical path = 2.0 cm, dose = 24.4 Gy. The solid line represents the first-order kinetic fit to the data.

Next we considered the reactivity of the reductant $Fe(CN)_6^{4-}$. Ar-purged solutions of 1 mM 8-Br-dAdo containing 0.25 M *t*-BuOH and different concentrations of $K_2Fe(CN)_6$ (25−100 μM) at pH 7 were used. No substantial changes were observed with respect to the experiment without the reductant. Indeed, only a slight decrease (4−5%) of the absorption at 360 nm was observed in comparison with the analogous reaction of Fe^{3+} salt (cf. inset of Figure 3). Under these conditions, the kinetics of formation and decay of transient absorbing at 360 nm were unaffected, suggesting slow reactions, if any, of the C5′ radical **2** and of the aminyl radical **3** with $Fe(CN)_6^{4-}$.

The reactivity of the weaker oxidant methyl viologen (MV^{2+}), $E°(MV^{2+}/MV^{•+}) = -0.45$ V,[37] with the transient species was also investigated. The experiments were performed by adding 50 or 100 μM MV^{2+} to Ar-purged solutions containing 1 mM 8-Br-dAdo and 0.25 M *t*-BuOH. Under these conditions, the competition between 8-Br-Ado and MV^{2+} for e_{aq}^- was comparable because $k(e_{aq}^- + MV^{2+}) = 7.2 \times 10^{10}$ M^{-1} s^{-1}.[25,30] Indeed, a two-component increase of the absorption at 605 nm, characteristic of the methyl viologen radical cation ($MV^{+•}$, $\epsilon_{605\ nm} = 1.37 \times 10^4$ M^{-1} cm^{-1}),[38] was observed upon irradiation. In particular, using 100 μM MV^{2+}, we found that the instan-

(32) Candeias, L. P.; Steenken, S. *J. Phys. Chem.* **1992**, *96*, 937−944.
(33) $k[HO• + i\text{-PrOH}] = 1.9 \times 10^9$ M^{-1} s^{-1} and $k[H• + i\text{-PrOH}] = 7.4 \times 10^9$ M^{-1} s^{-1}.[25,30]
(34) Buxton, G. V.; Mulazzani, Q. G. In *Electron Transfer in Chemistry*; Balzani, V., Ed.; Wiley-VCH: Weinheim, 2001; Vol. 1, p 549. For applications to analogous radicals, see refs 28, 32, and 36.
(35) Hausler, K. E.; Lorenz, W. J. In *Standard Potentials in Aqueous Solution*; Bard, A. J., Parsons, R., Jordan, J., Eds.; Marcel Dekker: New York, 1985; p 408.
(36) Candeias, L. P.; Wolf, P.; O'Neill, P.; Steenken, S. *J. Phys. Chem.* **1992**, *96*, 10302−10307.
(37) Wardman, P. *J. Phys. Chem. Ref. Data* **1989**, *18*, 1637−1755 and references therein.
(38) Watanabe, T.; Honda, K. *J. Phys. Chem.* **1982**, *86*, 2617−2619.

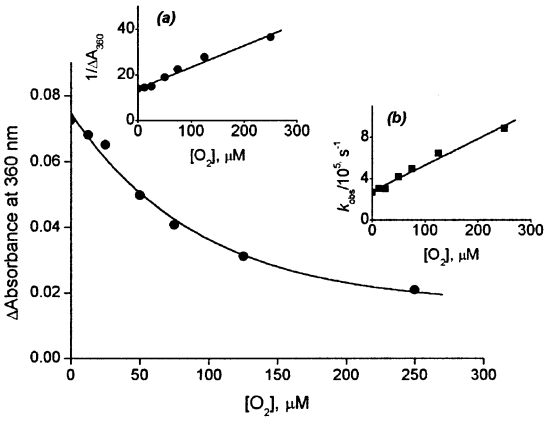

Figure 5. Dependence of ΔAbsorbance at 360 nm on $[O_2]$ obtained from the pulse radiolysis of solutions containing 1 mM 8-Br-dAdo and 0.25 M *t*-BuOH at pH ≈ 7 saturated with Ar/O_2 mixtures; optical path = 2.0 cm, dose = 17 Gy. The solid line represents an exponential fit to the data. Insets: (a) Dependence of 1/ΔAbsorbance at 360 nm on $[O_2]$. (b) Dependence of k_{obs} for growth at 360 nm on $[O_2]$.

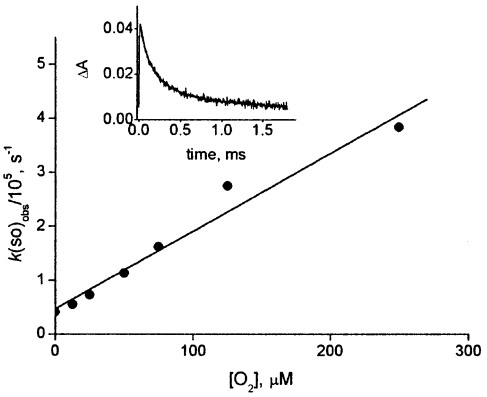

Figure 6. Dependence of k_{obs} for second-order decay at 360 nm obtained from the pulse radiolysis of solutions containing 1 mM 8-Br-dAdo and 0.25 M *t*-BuOH at pH ≈ 7 saturated with Ar/O_2 mixtures. Inset: Time dependence of ΔAbsorbance at 360 nm in the presence of 75 mM O_2; optical path = 2.0 cm, dose = 17 Gy. The solid line represents a second-order kinetic fit to the data.

taneous formation of $MV^{+\bullet}$ accounted for 32% of e_{aq}^-, whereas the slow growth accounted for 12%. Because the $Me_2C(OH)$-$CH_2^\bullet$ radical does not react with MV^{2+}, this demonstrates an electron transfer between the precursor of aminyl radical **3** (i.e., C5′ radical) and MV^{2+} with a rate constant of 2.2×10^8 M^{-1} s^{-1}. It is also worth mentioning that under these conditions the $MV^{\bullet+}$ decays by second-order kinetics ($k_{obs} = 2.4 \times 10^9$ M^{-1} s^{-1}), which probably involves an electron going back to the aminyl **3** or to the $Me_2C(OH)CH_2^\bullet$ radical.

The reactivity of molecular oxygen was investigated by pulsing solutions of 1 mM 8-Br-dAdo containing 0.25 M *t*-BuOH and different concentrations of O_2 (0−250 μM) at pH 7. The absorption at 360 nm was found to decrease by increasing the concentration of O_2 (Figure 5). For this decrease, the reactions of e_{aq}^- with 8-Br-dAdo and O_2 should be considered, because $k[e_{aq}^- + O_2] = 1.9 \times 10^{10}$ M^{-1} s^{-1}.[25,30] Taking into consideration the percentage of e_{aq}^- captured by O_2 and using a Stern−Volmer type of approach (inset a), we obtained $k_{oxygen}/k_c = 6.9 \times 10^3$ M^{-1}. A combination of these data with the k_c value yielded $k_{oxygen} = 1.1 \times 10^9$ M^{-1} s^{-1}. On the other hand, the first-order growth (k_{obs}) increased linearly by increasing the oxygen concentration, that is, $k_{obs} = k_c + k_{oxygen}[O_2]$. From the slope of k_{obs} versus $[O_2]$, the bimolecular rate constant was found to be 2.5×10^9 M^{-1} s^{-1} (inset b). An average value of $k_{oxygen} = (1.8 \pm 1) \times 10^9$ M^{-1} s^{-1} is suggested for the reaction of the C5′ radical **2** with molecular oxygen.

The presence of O_2 also influenced the disappearance of radical **3**. The second-order kinetics became faster as the concentration of O_2 increased. Figure 6 shows the dependence of k_{obs} on $[O_2]$, and the inset shows the second-order kinetic fit to the data for 75 μM of oxygen. Such a behavior is consistent with the reversible reaction of aminyl radical **3** with O_2 to give the corresponding peroxyl adduct (eq 3/−3), followed by cross-termination between this radical with a second radical **3** (eq 4). Under these conditions, the second-order rate constant, $k(so)_{obs}$, will be faster and a complex function of $[O_2]$, k_3, k_{-3}, and k_4.[39]

$$\mathbf{3}^\bullet + O_2 \rightleftharpoons \mathbf{3}\text{−}OO^\bullet \qquad (3/-3)$$

$$\mathbf{3}\text{−}OO^\bullet + \mathbf{3}^\bullet \rightarrow \text{products} \qquad (4)$$

Table 1. Rate Constants for the Reaction of the 2′-Deoxyadenosin-5′-yl Radical and the 1,2-Dihydroxyethyl Radical[a]

	rate constant (M^{-1} s^{-1})	
trapping agent	2′-deoxyadenosin-5′-yl	$HOCH(\bullet)CH_2OH$[b]
oxygen	$(1.8 \pm 1) \times 10^9$	3.2×10^9
$Fe(CN)_6^{3-}$	$(4.2 \pm 0.4) \times 10^9$	3.6×10^9
MV^{2+}	$(2.2 \pm 0.4) \times 10^8$	1.8×10^8

[a] Reactions in neutral water at (22 ± 2) °C. [b] Data from ref 40; see also ref 30.

Table 2. Rate Constants for the Reactions of Aminyl Radicals **3**, **6**, and **7**[a]

	rate constant (M^{-1} s^{-1})		
trapping agent	radical **3**	radical **6**[d]	radical **7**[e]
oxygen	*b*		3.3×10^8
$Fe(CN)_6^{3-}$	$(8.3 \pm 0.3) \times 10^8$		5.9×10^8
MV^{2+}	*c*	$<10^7$	$<10^7$

[a] Reactions in neutral water at (22 ± 2) °C. [b] See text. [c] Reaction not observed. [d] Data from ref 32. [e] Data from ref 36.

Table 1 summarizes the results obtained for the trapping of 2′-deoxyadenosin-5′-yl radical (**2**), together with the analogous reactions of the $HOCH(\bullet)CH_2OH$ radical produced from ethylene glycol. The reactivities of the two species toward oxygen and oxidants are very similar. The rate constants for the reactions with oxygen are typical for α-heteroatom substituted alkyl radicals.[30,40] The rate constants for the reactions with MV^{2+} are at least 1 order of magnitude slower than those with the stronger oxidant $Fe(CN)_6^{3-}$, which probably involve an inner-sphere electron-transfer process.[41]

Table 2 summarizes the results obtained for the trapping of aminyl radical **3**. For comparison, the analogous values for the reactions of isostructural radicals **6** and **7** are also given. The reactivity of the most structurally similar radical **6** is unfortunately limited to the reaction with MV^{2+}. Indeed, MV^{2+} is not

(39) For kinetic details of a similar mechanistic scheme, see: Kelly, C. A.; Blinn, E. L.; Camaioni, N.; D'Angelantonio, M.; Mulazzani, Q. G. *Inorg. Chem.* **1999**, *38*, 1579−1584 and 2756.
(40) Adams, G. E.; Willson, R. L. *Trans. Faraday Soc.* **1969**, *65*, 2981−2987. Steenken, S.; Davies, M. J.; Gilbert, B. C. *J. Chem. Soc., Perkin Trans. 2* **1986**, 1003−1010.
(41) Grodkowski, J.; Neta, P.; Schlesener, C. J.; Kochi, J. K. *J. Phys. Chem.* **1985**, *89*, 4373−4378.

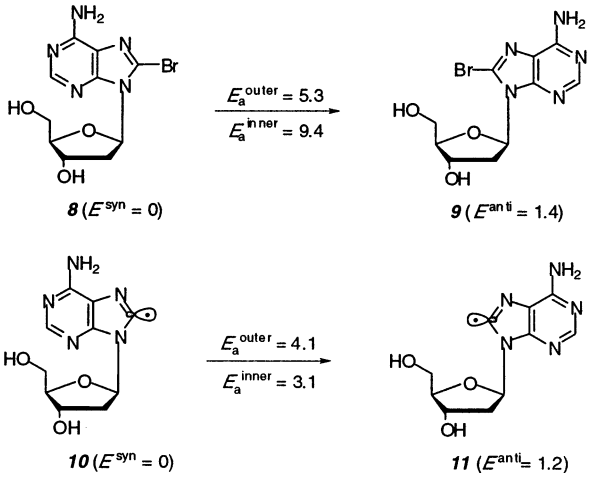

Figure 7. Relative stabilities of syn and anti conformers (*E*, kcal/mol) together with the outer and inner rotational barriers about the *N*-glycosidic bonds (E_a, kcal/mol) at the UB3LYP/6-31G* level. Values corrected for the difference in ZPVE (cf. ref 42).

able to oxidize fast enough any of these radicals.[32,36] On the other hand, it is gratifying to see the similarity of the behavior of radicals **3** and **7** toward the stronger oxidant $Fe(CN)_6^{3-}$. Because $E°[Fe(CN)_6^{3-}/Fe(CN)_6^{4-}] = 0.36$ V,[35] the $E°(\mathbf{5}^{+}/\mathbf{3}^{\bullet})$ should be ≤ 0.36 V. Moreover, the rate constant observed for the decay of $MV^{+\bullet}$ might be attributed to the reaction with the aminyl radical **3**. $MV^{+\bullet}$ is a stronger reductant than $Fe(CN)_6^{4-}$ and perhaps is able to reduce the aminyl radical **3**. Because $E°(MV^{2+}/MV^{\bullet+}) = -0.45$ V,[37] the $E°(\mathbf{3}^{\bullet}/\mathbf{3}^{-})$ should be ≥ -0.45 V.

MO Calculations. MO calculations with the DFT method were performed to determine the factors that affect the activation energies of the suggested reactions.[42,43] Initially, B3LYP/6-31G* calculations were carried out on 8-Br-dAdo in the syn (**8**) and anti (**9**) conformation (Figure 7). The syn conformer is computed to be more stable than the anti as was found experimentally. This finding was ascribed to the presence of the bulky Br atom. The vertical electron affinities (VEA) of the more stable syn conformer (**8**) are estimated to be negative (−0.9 eV) at the B3LYP/6-31G* level so that the radical anion could be unstable in the gas phase.[44] Interestingly, when the structural parameters of the radical anion were optimized, the radical anion of **8** lost Br^{-}, producing the neutral σ-type radical **10** in accordance with

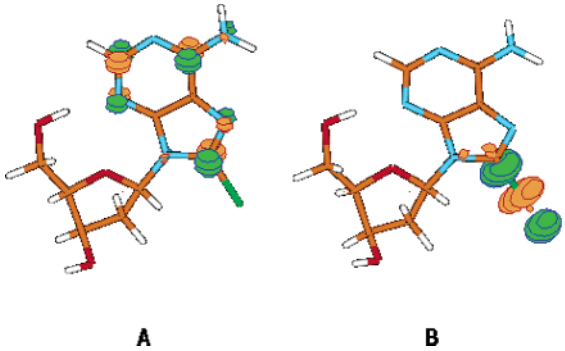

Figure 8. SOMO (A) and LUMO (B) of the electron adduct 8-Br-dAdo$^{-\bullet}$ computed at the geometry of 8-Br-dAdo at the UB3LYP/6-31G* level.

experimental evidence. Indeed, electron distribution in the SOMO of the radical anion computed at the geometry of the neutral molecule (Figure 8A) shows that the unpaired electron is mainly localized in the five-membered ring at C8, that is, at the carbon linked to the Br atom. The lowest unoccupied MO (LUMO) of the anion lies only 1.5 eV at higher energy than the SOMO and is localized at the C8−Br bond being antibonding in character (Figure 8B). Thus, the unpaired electron tends to occupy the antibonding σ^*_{C8-Br} MO upon relaxing the structural parameters, favoring the loss of Br^{-}.

DFT calculations were then performed to determine the rotational barriers about the *N*-glycosidic bond in both the 8-Br-dAdo (**8**,**9**) and the C8 radical of σ-type (**10**,**11**). Figure 7 shows the relative stabilizations of the syn and anti conformers as well as the rotational barriers for the two available paths (outer and inner) of the interconversion between the two conformers. The inner refers to the rotation in which the Br moiety or the radical center passes above the sugar ring and the outer to the opposite direction. In both systems, the syn conformer is more stable than the anti of 1.2−1.4 kcal/mol. The comparison of the two rotational paths for the conversion of **8** to **9** shows that the inner rotation is more crowded and, therefore, requires a higher barrier. After the removal of Br atom, the inner rotation barrier for the conversion of **10** to **11** considerably decreases due to the lower steric demand. Therefore, the conformer **11** is substantially populated.

Next we considered the radical translocation from the C8 to the position C5′. In the transition state for such a hydrogen abstraction, the C8···H···C5′ have to be collinear or nearly so. The two conformers around the C4′−C5′ bond (**12** and **13**), which differ in stability by 1.2 kcal/mol, have this arrangement (Figure 9). The radical translocations of both conformers are exothermic of ca. 20 kcal/mol as expected on the thermochemical grounds[21] and occur with a reaction barrier of ca. 3 kcal/mol to give the C5′ radical of π-type, which is nearly planar with a very low interconversion barrier. The conformers **14** and **15** of the C5′ radical have essentially the same stability.

Chart 1 shows the four possible aminyl radicals, which can be obtained for the cyclization of radicals **14** and **15**. Cyclization of radical **14** is expected to produce radicals **16** and **17**, that is, (5′*R*)-isomers, which have a defined stereochemistry also at position C8 derived from the *back* or *front* attack, respectively. Analogously, cyclization of radical **15** is expected to produce radicals **18** and **19**, that is, (5′*S*)-isomers, derived again from the *back* or *front* attack, respectively. The UB3LYP/6-31G* calculations have been extended to the cyclization of radical

(42) DFT calculations were carried out with the Gaussian 98 system of programs[43] running on DEC-Alpha 500 computers employing the B3LYP functional and the valence double-ζ basis set supplemented with polarization *d*-function on heavy atoms (B3LYP/6-31G*). The unrestricted wave function was used for radical species (UB3LYP/6-31G*). The nature of the transition states was verified by frequency calculations (one imaginary frequency), and energy values were corrected for the zero-point vibrational energy (ZPVE).

(43) Frisch, M. J.; Trucks, G. W.; Schlegel, H. B.; Scuseria, G. E.; Robb, M. A.; Cheeseman, J. R.; Zakrzewski, V. G.; Montgomery, J. A., Jr.; Stratmann, R. E.; Burant, J. C.; Dapprich, S.; Millam, J. M.; Daniels, A. D.; Kudin, K. N.; Strain, M. C.; Farkas, O.; Tomasi, J.; Barone, V.; Cossi, M.; Cammi, R.; Mennucci, B.; Pomelli, C.; Adamo, C.; Clifford, S.; Ochterski, J.; Petersson, G. A.; Ayala, P. Y.; Cui, Q.; Morokuma, K.; Malick, D. K.; Rabuck, A. D.; Raghavachari, K.; Foresman, J. B.; Cioslowski, J.; Ortiz, J. V.; Stefanov, B. B.; Liu, G.; Liashenko, A.; Piskorz, P.; Komaromi, I.; Gomperts, R.; Martin, R. L.; Fox, D. J.; Keith, T.; Al-Laham, M. A.; Peng, C. Y.; Nanayakkara, A.; Gonzalez, C.; Challacombe, M.; Gill, P. M. W.; Johnson, B.; Chen, W.; Wong, M. W.; Andres, J. L.; Gonzalez, C.; Head-Gordon, M.; Replogle, E. S.; Pople, J. A. Gaussian 98, revision A.7; Gaussian, Inc.: Pittsburgh, PA, 1998.

(44) Diffuse functions were not added to the basis set to better describe the radical anion because in this case the calculations could provide unreliable results for unstable anions, see: Guerra, M. *Chem. Phys. Lett.* **1990**, *167*, 315−319. Guerra, M. *J. Phys. Chem. A* **1999**, *103*, 5983−5988.

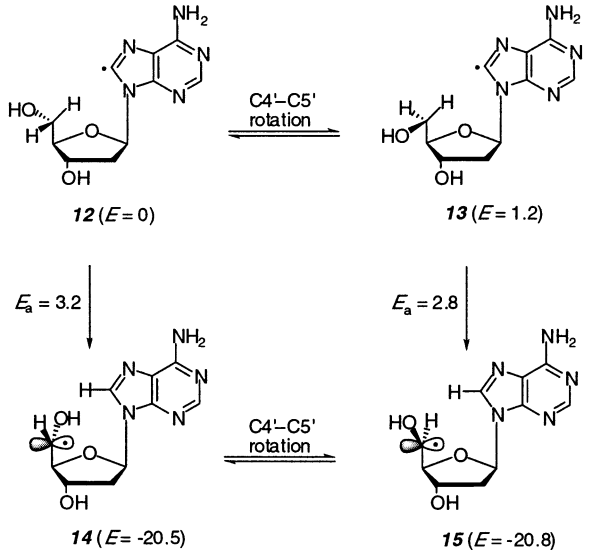

Figure 9. Relative stabilities (E, kcal/mol) of the two σ-type radical conformers (**12**,**13**) and of the two π-type radical conformers (**14**,**15**) together with the activation energies for the radical translocation (E_a, kcal/mol) at the UB3LYP/6-31G* level. Values are corrected for the difference in ZPVE.

Chart 1

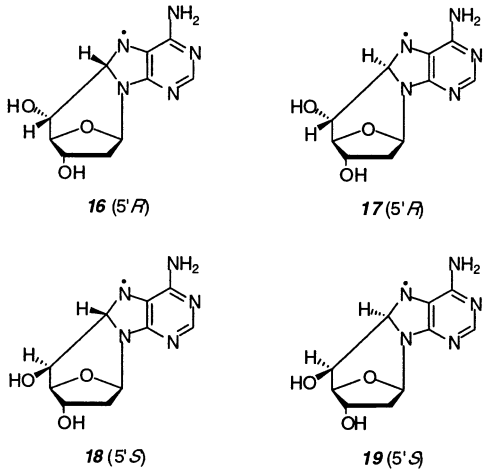

Table 3. Reaction Barriers (E_a), Reaction Enthalpies (H_r), Partial Bond Lengths (d_{TS}), and Angle of Attacks (ϕ_{TS}) in the Transition States for the Cyclizations of Radicals **14** and **15** Computed at the UB3LYP/6-31G* Level[a]

cyclization	ring formation	E_a, kcal/mol	H_r, kcal/mol	d_{TS}, Å	ϕ_{TS}, deg
14 → **16**	chair	8.4	−9.3	2.229	108.6
14 → **17**	boat	13.3	−4.9	2.181	113.3
15 → **18**	chair	13.5	−11.0	2.238	110.4
15 → **19**	boat	16.3	−6.9	2.202	110.2

[a] E_a and H_r values corrected for the difference in ZPVE (cf. ref 42).

C5′. Table 3 shows the values of reaction barriers (E_a), reaction enthalpies (H_r), partial bond lengths (d_{TS}), and angle of attacks (ϕ_{TS}) in the transition states. Figures 10A and 11A show the transition states of radical **14** for the *back* or *front* attacks, respectively. Figures 10B and 11B show the corresponding product radicals **16** and **17**. The *back* attack induced the chair conformation in the forming ring (Figure 10), whereas in the *front* attack the ring adopts a boat conformation (Figure 11). The reaction enthalpies (H_r) for the formation of aminyl radicals in the chair conformation (**16** and **18**) are almost twice as

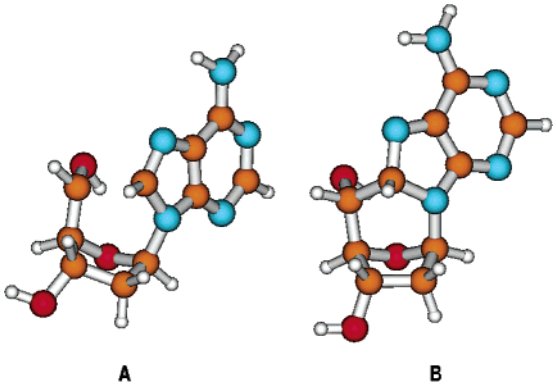

Figure 10. Geometries of the chair transition state (A) and product radical (B) for the *back* attack of radical **14** at the UB3LYP/6-31G* level.

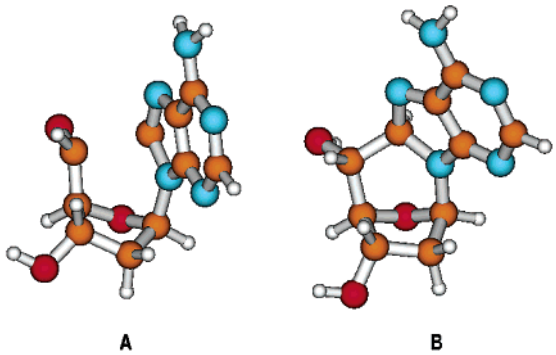

Figure 11. Geometries of the boat transition state (A) and product radical (B) for the *front* attack of radical **14** at the UB3LYP/6-31G* level.

exothermic as the corresponding H_r values of the boat forming radicals **17** and **19**. The angle of attack ϕ_{TS} in the transition states of **14** and **15** is close to the normal (109.47°), indicating that the dispositions of the three interactive atoms, that is, C5′–C8–N7, in all cyclizations are close to the stereoelectronic requirements according to the Baldwin–Beckwith set of empirical rules.[45] On the other hand, the barriers of transition states in the chair arrangements (**14** → **16** and **15** → **18**) are 3–5 kcal/mol lower than those of the corresponding boat due to the hydrogen bondings with the oxygen in the sugar ring (2.18 and 2.70 Å, respectively) (Figures 10A and 11A). Therefore, the reaction enthalpies and the hydrogen bondings of HO5′ in the chair transition states play an important role in determining the small size of the reaction barrier in the cyclization **14** → **16**.

Figure 12 summarizes the progress of reaction from radical **12** to radical **16** via the intermediacy of the C5′ radical **14** (solid line). That is, the barriers of 3.2 and 8.4 kcal/mol are needed for the radical translocation and the cyclization steps, respectively. The exothermicity of this stepwise reaction (**12** → **14** → **16**) is 29.8 kcal/mol. However, the possibility of a "concerted" mechanism can also be considered. After the TS, during the path downhill to **14** there could be a point where the two moieties (i.e., purine and C5′ radical) are very close to the optimum geometry of the transition state for cyclization. Instead of relaxing from the crest to give radical **14**, they could undertake the uphill with much less barrier. Calculations showed that if the cyclization is forced at this stage assuming the C5′–C8 as reaction coordinate (see **20** in Figure 12), the reaction

(45) Baldwin, J. E. *J. Chem. Soc., Chem. Commun.* **1976**, 734–736. Beckwith, A. L. J.; Easton, C. J.; Serelis, A. K. *J. Chem. Soc., Chem. Commun.* **1980**, 482–483.

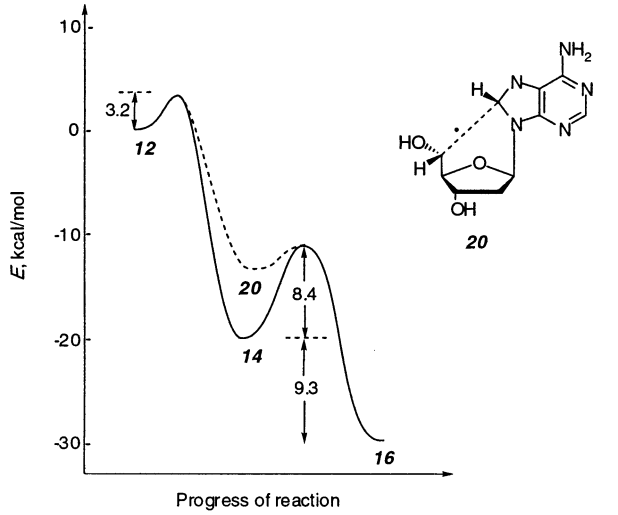

Figure 12. Progress or reaction in a stepwise (**12** → **14** → **16**) or concerted (**12** → **20** → **16**) mechanism.

Table 4. Vertical Optical Transitions (Wavelengths λ, Oscillator Strengths *f*) for Aminyl Radical **16** Computed at the UB3LYP/6-311+G*//UB3LYP/6-31G* Level with the TD-DFT Method along with Experimental λ_{max} Values[a]

λ, nm	f	transition {spin}	exp, nm
440	0.017	pπ(out-of-phase N1,N3) → SOMO(N7) {β}	470
350	0.093	SOMO(N7) → π*(N1−C2) {α}	360
320	0.068	lone pair NH_2 → SOMO(N7) {β}	
300	0.052	pπ(N9) → SOMO(N7) {β}	

[a] Only transitions with *f* greater than 0.005 are reported.

barrier drops from 8.4 to 2.3 kcal/mol (dashed line). However, **20** is not a true minimum of the hypersurface. That is, relaxing the C5′−C8 constrain **20** gives radical **14**. Similarly, E_a values of 13.3, 13.5, and 16.5 kcal/mol in Table 3 drop to 5.2, 6.3, and 6.8 kcal/mol, respectively.

The optical spectrum (transition wavelength λ and oscillator strength *f*) of the aminyl radical **16** was computed with the time-dependent DFT method which was shown to reproduce the UV−vis spectra of radicals fairly well.[46] Table 4 shows that the theoretical results (TD-UB3LYP/6-311+G*//UB3LYP/6-31G*) are in good accordance with experiment, the transition energy being overestimated by about 0.15 eV. The higher intensity transition was computed at 350 nm, that is, very close to the strong maximum observed at 360 nm in the pulse radiolysis experiment. Calculations indicate that this transition is due to an excitation from the SOMO localized to the pπ orbital of N7 to the antibonding π* of the N1−C2 double bond (α spin transition). Calculations also suggest that this broad band that extends to λ < 300 nm could probably originate from the overlapping of three transitions. The other two transitions are computed to occur at lower wavelengths (320 and 300 nm) and involve electron transfer from the N lone pair of the amino group and from the pπ orbital of the nitrogen (N9) of the glycosyl link to the SOMO (β spin transition). Transition from the out-of-phase mixing of the pπ N1 and N3 orbitals to the SOMO is computed to occur at higher wavelengths (440 nm) and should be responsible for the weak absorption observed in the visible region during pulse radiolysis at 470 nm.

Product Studies. A deareated aqueous solution (1 L) containing 1.5 mM of 8-Br-dAdo (495 mg), 0.25 M *t*-BuOH, and 4 mM $K_4Fe(CN)_6$ at pH ≈ 7 was γ-irradiated with a total dose up to 3 kGy at a dose rate of 18 Gy/min. The crude reaction mixture was passed through ion-exchange resin (Amberlite IRA-400) to eliminate the iron salts. The HPLC analysis of the reaction mixture showed that the starting bromide was consumed 55% and that several products were formed, one of which predominates.[49] Workup of the reaction mixture and separation by RP silica gel chromatography afforded the major product (5′*R*)-5′,8-cyclo-dAdo (**21**) in a 61% yield (based on the recovered starting bromide). Some of the minor products could be isolated as pure materials. The 5′,8-cyclo-2′,5′-dideoxyAdo (**23**) and (5′*S*)-5′,8-cyclo-dAdo were spectroscopically characterized and together with adenine and dAdo were used for calibration of the quantitative HPLC analysis (see below).

The isolation of (5′*R*)- and (5′*S*)-isomers was previously obtained by semipreparative HPLC, and a not very well-resolved ^{1}H NMR (200 MHz) was reported in D_2O.[15,24] In the Experimental Section, a detailed NMR characterization is reported for both compounds. In particular, proton NMR (400 MHz) spectra in both D_2O and DMSO are compared. In D_2O, the chemical shifts are shifted 0.2−0.4 ppm upfield as compared to DMSO and ca. 0.1 downfield as compared to the data reported in the literature. It is worth mentioning that the $J_{4'5'}$ is zero (in DMSO) or 1.2 Hz (in D_2O) for the (5′*R*)-isomer and 6.0−6.1 Hz for the (5′*S*)-isomer in both solvents. Structural information of (5′*R*)-isomer **21** was also obtained from multiple fragmentation experiments using ESI-Ion Trap MS^n. The MS^1 spectrum consisted of the protonated molecular ion (MH^+) at *m*/*z* 250, whereas the MS^2 spectrum showed three daughter ions. The two ions at *m*/*z* 232 and 214 should be related to the loss of one and two water molecules from the parent ion, respectively. The third one at *m*/*z* 164 can be assigned to the base fragment resulting from the cleavages of the glycosidic and C4′−C5′ bonds.[50] Indeed, the MS^3 spectrum of this ion leads to *m*/*z* 136 (protonated adenine) by the loss of a CO group.

Additional experiments were performed to obtain further mechanistic information for this synthetically useful radical cascade process. The dose profile of the reaction is followed by HPLC with 3 mL scale experiments, and the products were quantified by comparison with the authentic samples. For example, the experiment with 1.5 kGy dose gave the following results (yields): adenine (5%), (5′*R*)-isomer **21** (60%), (5′*S*)-isomer (10%), dAdo (7%), and compound **23** (7%). Yields are based on the consumption of 8-Br-dAdo. It is satisfying to see

(46) Good results were previously obtained using both triple ζ basis sets[47] (TD-UB3LYP/6-311G**//UHF/6-31G*) and double ζ basis sets plus diffuse functions (TD-UBLYP/6-31+G*//UBLYP/6-31G*).[48] The values reported in Table 2 have been computed with the more flexible 6-311+G* basis set (TD-UB3LYP/6-311+G*//UB3LYP/6-31G*). Interestingly, the transition wavelengths differ less than 0.05 nm from those computed with smaller basis sets (TD-UB3LYP/6-311G**//UB3LYP/6-31G*, TD-UB3LYP/6-31+G*//UB3LYP/6-31G*).

(47) Chatgilialoglu, C.; Ferreri, C.; Bazzanini, R.; Guerra, M.; Choi, S.-Y.; Emanuel, C. J.; Horner, J. H.; Newcomb, M. *J. Am. Chem. Soc.* **2000**, *122*, 9525−9533.

(48) Weisman, J. L.; Head-Gordon, M. *J. Am. Chem. Soc.* **2001**, *123*, 11686−11694.

(49) A detailed dose profile of 8-Br-dAdo consumption and (5′*R*)-isomer formation obtained by HPLC analysis showed that the total dose of 3kGy is the optimum for the product isolation (i.e., high conversion and less secondary products). The fact that ca. 55% of the starting bromide is consumed under these conditions indicates that ca. 85% of the produced solvated electrons and hydrogen atoms react with 8-Br-dAdo.

(50) The ESI-mass spectrum of (5′*R*)-isomer **21** was previously obtained from the analysis of the reaction mixture of the HO• radical with dAdo using a quadrupole and was discussed in detail.[2] The fragmentation pattern consisted of an ion at *m*/*z* 164 which has been unequivocally assigned to this fragmentation.

Scheme 4

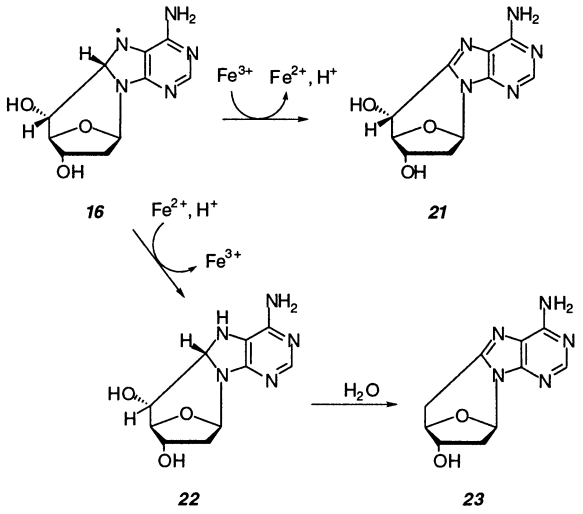

that the ratio (5′*R*):(5′*S*) = 6:1 is identical to that reported in the photolysis of 8-Br-dAdo.[24]

The disappearance of the starting material (mol kg^{-1}) divided by the absorbed dose (1 Gy = 1 J kg^{-1}) gives the radiation chemical yield or *G*[-(8-Br-dAdo)]. A plot of *G*[-(8-Br-dAdo)] versus dose and extrapolation of the line to zero dose gives a *G*[-(8-Br-dAdo)] = 0.32 which is close to the sum $G(e_{aq}^-)$ + $G(H^\bullet)$ = 0.27 + 0.06 = 0.33. These findings lead to the conclusion that the solvated electrons and the hydrogen atoms react almost quantitatively with 8-Br-dAdo. The analogous reaction without $K_4Fe(CN)_6$ afforded **21** in 25% yield. Under these conditions, it was possible to identify and quantify Br^- by comparison with KBr (the HPLC analysis monitored at 210 nm).[23] It is gratifying to see that the radiation chemical yield for the formation of bromide was equal to the consumption of starting compound. With regards to the latter experiment, when $K_4Fe(CN)_6$ was added to the reaction mixture after its irradiation, and after a standing time equal to the irradiation time, no changes were detected with respect to the product yields. The absence of the post-irradiation effect means that the iron salts must be involved in the free radical transformation. Furthermore, the formation of $K_3Fe(CN)_6$, which can be conveniently monitored by UV−vis spectroscopy at 420 nm (ϵ = 1020 M^{-1} cm^{-1}),[51] in steady-state experiments was found to be negligible.

Taken into consideration the pulse radiolysis and computational data for the fate of e_{aq}^-, the cyclization of the C5′ radical should afford mainly the aminyl radical **16** with the defined stereochemistry at the C5′ and C8 positions (Scheme 4). On the basis of the pulse radiolysis results, $Fe(CN)_6^{3-}$ generated in situ (see below) can easily oxidize radical **16** to give compound **21**. Analogously, radical **17** can afford the same compound **21**, whereas the radical **18** should give the corresponding (5′*S*)-isomer (cf. Chart 1 and Table 3).[52] The radical **16** may be also reduced slowly by $Fe(CN)_6^{4-}$ followed by fast protonation to give compound **22**, which can readily eliminate H_2O (the OH group in the 5′ position being in anti arrangement with the H atom in the 8 position) and give the cyclonucleoside **23** after tautomerization (Scheme 4).

Scheme 5

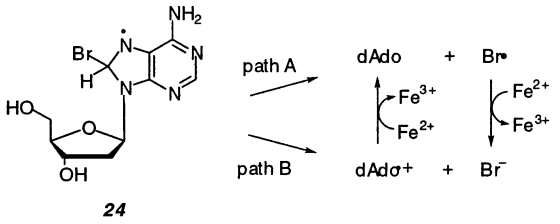

Scheme 5 shows some possible mechanistic paths for the formation of dAdo by rationalization of the experimental data. The hydrogen atom might add to the C8,N7 double bond of the starting bromide to give the radical **24**. This radical could either lose rapidly $Br^\bullet$ to afford dAdo (path A) or cleave heterolytically to give the radical cation of 2′-deoxyadenosine and Br^- (path B). In their turn, $Br^\bullet$ or $dAdo^{\bullet+}$ can react with $Fe(CN)_6^{4-}$ to give Br^- or dAdo. Alternatively, an adduct that derived from the reaction of $H^\bullet$ with $Fe(CN)_6^{4-}$ (see below) might be able to react with 8-Br-dAdo to give dAdo by unknown chemistry. The mechanism of the adenine formation is unclear at present.

The role of $K_4Fe(CN)_6$ is discussed next. In the presence of 0.25 M *t*-BuOH and 4 mM $K_4Fe(CN)_6$, the attack of $HO^\bullet$ radicals occurs in about 80% of the cases at the *t*-BuOH (eq 2) and in about 20% of the cases at the $K_4Fe(CN)_6$, $k[HO^\bullet + Fe(CN)_6^{4-}] = 1.0 \times 10^{10}$ M^{-1} s^{-1}.[25,30] Therefore, the reaction of $HO^\bullet$ with $Fe(CN)_6^{4-}$ will contribute to the formation of oxidant $Fe(CN)_6^{3-}$. It is also reported that $Fe(CN)_6^{4-}$ reacts with $H^\bullet$ with a rate constant of 3.9×10^7 M^{-1} s^{-1} to give an unknown adduct.[53] The latter could be a reactive species toward the observed transients or might transform to $Fe(CN)_6^{3-}$. Probably the $H^\bullet$ atoms are partitioned between the two reaction channels, that is, addition to 8-Br-dAdo and to $Fe(CN)_6^{4-}$. It is worth also mentioning that $Fe(CN)_6^{3-}$ reacts with $H^\bullet$ to regenerate $Fe(CN)_6^{4-}$ ($k = 6.0 \times 10^9$ M^{-1} s^{-1}) and the carbon-centered radical generated from eq 2 is also reported to react with $Fe(CN)_6^{3-}$ ($k = 3.0 \times 10^6$ M^{-1} s^{-1})[25,30] and probably affords $Fe(CN)_6^{4-}$.[36] In summary, a steady-state concentration at the micromolar level of oxidant(s) should be present during the course of these reactions.

Conclusions

DNA radicals have attracted the interest of chemists and biochemists for years, and there is a large body of results for the involvement of C5′ radicals.[6,11,54] In this paper, we studied the chemistry of model C5′ DNA radicals and in particular of the 2′-deoxyadenin-5′-yl radical with the aim of determining the structural and reactivity effects regarding the formation of the 5′,8-cyclonucleoside as well as the redox properties of the two participating radicals in this cyclization. We found that the C5′ radical adds intramolecularly to the C8,N7 double bond of the adenine moiety with a rate constant of 1.6×10^5 s^{-1} at room temperature. This process is highly stereospecific, and UB3LYP/G-31G* calculations suggest that from the four possible paths, the one with a chair conformation and *R*-configuration at the C5′ position in the forming ring has the

(51) Schuler, R. H.; Hartzell, A. L.; Behar, B. *J. Phys. Chem.* **1981**, *85*, 192−199.
(52) The relative yields of (5′*R*)- and (5′*S*)-isomers suggest that the gap between the activation energies for the cyclization of radicals **14** and **15** via the chair conformation must be much smaller than the difference of calculated energy barriers (cf. Table 3).
(53) Zehavi, D.; Rabani, J. *J. Phys. Chem.* **1974**, *78*, 1368−1373.
(54) For example, see: Goldberg, I. H. *Acc. Chem. Res.* **1991**, *24*, 191−198. Nicolaou, K. C.; Dai, W.-M. *Angew. Chem., Int. Ed. Engl.* **1991**, *30*, 1387−1416. Pratviel, G.; Bernadou, J.; Meunier, B. *Angew. Chem., Int. Ed. Engl.* **1995**, *34*, 746−769.

lowest reaction barrier. The rate constants for the reactions of the C5′ radical with O_2, Fe^{3+}, and MV^{2+} are similar to those reported for the 1,2-dihydroxyethyl radical and typical of other sugar radicals in the 2′-deoxyribo series.[47] On the other hand, the aminyl radical **3** adds reversibly to molecular oxygen and accepts electrons only from the strongest oxidant (Fe^{3+}). Taking advantage of the observed reactivities, we developed a synthetically useful one-pot procedure that allows for the conversion of 8-Br-dAdo to 5′,8-cyclo-dAdo in a diastereoisomeric ratio (5′*R*):(5′*S*) = 6:1.

From a biological perspective, the main reactions of the 2′-deoxyadenin-5′-yl radical in DNA are cyclization, repair reaction by hydrogen abstraction from glutathione, and trapping by O_2 to give the corresponding peroxyl radical.[6,54] Assuming the rate constant for the cyclization of 2′-deoxyadenin-5′-yl radical in DNA is close to 10^5 s^{-1} as seen from the present study, we deduced that both the repair reaction by glutathione (at the millimolar level in biological systems)[55] and the trapping by O_2 (at the micromolar level) would compete with cyclization.[56] However, it is worth recalling that the diastereoisomeric ratio (5′*R*):(5′*S*) of 5′,8-cyclo-dAdo moieties in both single- and double-stranded DNA are approximately 2.[1,2] Using the data obtained from the present study, we suggested that restricted conformations due to the supramolecular organization should contribute to decreasing considerably the cyclization rate constant, due to both enthalpic and entropic effects. Indeed, it has already been observed that the 5′,8-cyclo-dAdo moieties decrease substantially upon irradiation of DNA in the presence of molecular oxygen.[1]

Experimental Section

Pulse Radiolysis. Pulse radiolysis with optical absorption detection was performed by using the 12 MeV linear accelerator, which delivered 20−200 ns electron pulses with doses between 5 and 50 Gy, by which $HO^•$, $H^•$, and e_{aq}^- are generated with 1−20 μM concentrations. The pulse irradiations were performed at room temperature (22 ± 2 °C) on samples contained in Spectrosil quartz cells of 2 cm optical path length. Solutions were protected from the analyzing light by means of a shutter and appropriate cutoff filters. The bandwith used throughout the pulse radiolysis experiments was 5 nm. The radiation dose per pulse was monitored by means of a charge collector placed behind the irradiation cell and calibrated with a N_2O-saturated solution containing 0.1 M HCO_2^- and 0.5 mM methyl viologen, using $G\epsilon = 9.66 \times 10^{-4}$ m^2 J^{-1} at 602 nm.[39] $G(X)$ represents the number of moles of species X formed or consumed per joule of energy absorbed by the system.

Continuous Radiolysis. Continuous radiolyses were performed at room temperature (22 ± 2 °C) on 10−100 mL samples using a ^{60}Co-Gammacell, with dose rates between 20 and 25 Gy min^{-1}. The absorbed radiation dose was determined with the Fricke chemical dosimeter, by taking $G(Fe^{3+}) = 1.61$ μmol J^{-1}.[57] The reactions of 8-Br-dAdo[58] with e_{aq}^- and $H^•$ were investigated using deareated aqueous solutions containing 1.5 mM substrate and 0.25 M *t*-BuOH in the presence or absence of 4 mM $K_4Fe(CN)_6$ at pH ≈ 7.

One liter of solution was irradiated with a total dose up to 3 kGy. The crude reaction mixture was passed through ion-exchange resin (Amberlite IRA-400) to eliminate the iron salts. The reaction mixture was then lyophilized, and the residue was taken up in water and purified on reverse-phase column chromatography equipped with a peristaltic pump, a UV detector (RP18, eluted in water with a 0−30% methanol nonlinear gradient over 5 h at a flow rate of 4 mL/min, detector at 260 nm). Two fractions were collected and lyophilized to give (5′*R*)-5′,8-cyclo-dAdo (**21**) in 61% and a mixture of some minor products in ca. 30% overall yield. Yields are based on the recovered starting bromide. 5′,8-Cyclo-2′,5′-dideoxyAdo (**23**) and (5′*S*)-5′,8-cyclo-dAdo were obtained as pure materials from the mixture of minor products repeatedly chromatographed on reverse-phase silica gel and spectroscopically characterized.

Alternatively, 3 mL solutions were irradiated at different doses. The crude reaction mixture was passed through ion-exchange resin (Amberlite IRA-400) to eliminate the iron salts and monitored by HPLC on a C18-reverse-phase column (Waters XTERRA, 150 × 4.6 mm, 5 μm), eluted in water with a 0−15 acetonitrile linear gradient over 30 min at a flow rate of 0.4 mL/min and detected at 254 nm. All products were identified and quantified by comparison with authentic samples. For example, the experiment with 1.5 kGy dose gave the following results in order of elution (retention time/min, yield): adenine (22.01, 5%), (5′*R*)-5′,8-cyclo-dAdo (22.96, 60%), (5′*S*)-5′,8-cyclo-dAdo (28.94, 10%), dAdo (29.92, 7%), and 5′,8-cyclo-2′,5′-dideoxyAdo (30.85, 7%). Yields are based on the 38% consumption of 8-Br-dAdo (retention time 40.64 min).

(5′*R*)-5′,8-Cyclo-2′-deoxyadenosine (21). ^{1}H NMR (400 MHz, D_2O reference peak 4.80 ppm): δ 8.18 (s, 1H, H2), 6.57 (d, 1H, $J_{1'2''} = 5.2$ Hz, H1′), 4.90 (d, 1H, $J_{5'4'} = 1.2$ Hz, H5′), 4.75 (d, 1H, $J_{4'5'} = 1.2$ Hz, H4′), 4.46 (dd, 1H, $J_{3'2'} = 7.6$ Hz, $J_{3'2''} = 3.6$ Hz, H3′), 2.59 (dd, 1H, $J_{2'2''} = -13.6$ Hz, $J_{2'3'} = 7.6$ Hz, H2′), 2.31 (dt, 1H, $J_{2''2'} = -13.6$ Hz, $J = 4.4$ Hz, H2″). ^{1}H NMR (400 MHz, DMSO-d_6): δ 8.08 (s, 1H, H2), 7.24 (s, 2H, NH_2), 6.41 (d, 1H, $J_{1'2''} = 4.4$ Hz, H1′), 6.18 (d, 1H, $J = 6.0$ Hz, OH5′), 5.43 (d, 1H, $J = 3.6$ Hz, OH3′), 4.59 (d, 1H, $J =$ 6.0 Hz, singlet after D_2O quenching, H5′), 4.43 (s, 1H, H4′), 4.19 (m, 1H, H3′), 2.26 (dd, 1H, $J_{2'2''} = -13.6$ Hz, $J_{2'3'} = 7.6$ Hz, H2′), 1.99 (dt, 1H, $J_{2''2'} = -12.8$ Hz, $J_{2''1'} = J_{2''3'} = 4.4$ Hz, H2″). ES-MS (positive mode): *m*/*z* 250 (MH^+). MS^2 (250): 232, 214, 164. MS^3 (164): 136.

5′,8-Cyclo-2′,5′-dideoxyadenosine (23). ^{1}H NMR (400 MHz, D_2O): δ 8.00 (s, 1H, H-2), 6.40 (d, 1H, $J_{1'2''} = 5.2$ Hz, H1′), 4.85 (d, 1H, $J_{4'5'} = 6.4$ Hz, H4′), 4.49 (dd, 1H, $J_{3'2'} = 7.2$ Hz, $J_{3'2''} = 3.2$ Hz, H3′), 3.45 (dd, 1H, $J_{5'5''} = -18.4$ Hz, $J_{5'4'} = 6.4$ Hz, H5′), 3.20 (d, 1H, $J_{5''5'} = -18.4$ Hz, H5″), 2.63 (dd, 1H, $J_{2'2''} = -14$ Hz, $J_{2'3'} = 7.2$ Hz, H2′), 2.26 (ddd, 1H, $J_{2''2'} = -14$ Hz, $J_{2''1'} = 5.2$ Hz, $J_{2''3'} = 3.2$ Hz, H2″). ES-MS (positive mode): *m*/*z* 234 (MH^+).

(5′*S*)-5′,8-Cyclo-2′-deoxyadenosine. ^{1}H NMR (400 MHz, DMSO-d_6): δ 8.06 (s, 1H, H2), 7.18 (s, 2H, NH_2), 6.35 (d, 2H, $J = 4.0$ Hz, H1′and OH5′, after D_2O quenching: d, 1H, $J_{1'2''} = 4.4$ Hz, H1′), 5.40 (d, 1H, $J = 4.8$ Hz, OH3′), 5.04 (dd, 1H, $J = 6.0$, 6.4 Hz, after D_2O quenching: d, 1H, $J_{5'4'} = 6.0$ Hz, H5′), 4.62 (m, 1H, H3′), 4.46 (d, 1H, $J_{4'5'} = 6.0$ Hz, H4′), 2.34 (dd, 1H, $J_{2'2''} = -13.2$ Hz, $J_{2'3'} = 7.6$ Hz, H2′), 2.03 (dt, 1H, $J_{2''2'} = -13.2$ Hz, $J_{2''1'} = J_{2''3'} = 4.4$ Hz, H2″). ES-MS (positive mode): *m*/*z* 250 (MH^+).

Acknowledgment. We are grateful to Roman Flyunt and Rita Bazzanini for their valuable contribution in the initial stage of the project.[23] We thank Clara Caminal i Comadira and Maria Duca for the help in the product isolation, and Carla Ferreri and M. Luisa Navacchia for valuable discussions. We also thank Angelo Monti and Alessandro Martelli for assistance with pulse radiolysis experiments. We are also grateful to Francesco Tortorella of Bruker Daltonics S.r.l. for the Ion Trap MS^n runs on an Esquire 3000 plus instrument.

JA029374D

(55) (a) The rate constant for the reaction of $CH_3CH(•)OH$ with glutathione is 1.1×10^8 M^{-1} s^{-1}.[25,30] (b) The intracellular level of glutathione in mammalian cells is in the 0.5−10 mM range, see: Meister, A.; Anderson, M. E. *Annu. Rev. Biochem.* **1983**, *52*, 711−760.
(56) The oxygen concentration is low in the nucleus, see: Zander, R. *Z. Naturforsch.* **1976**, *31C*, 339−352. Zander, R. *Adv. Exp. Med. Biol.* **1976**, *75*, 463−467.
(57) Spinks, J. W. T.; Woods, R. J. *An Introduction to Radiation Chemistry*, 3rd ed.; Wiley: New York, 1990; p 100.
(58) 8-Br-dAdo was purchased from Berry&Associates, Inc.